AGU PUBLICATIONS

JGR

Journal of Geophysical Research: Biogeosciences

RESEARCH ARTICLE
10.1002/2016JG003589

Key Points:
- Variability in P limitation indicated by nutrient stoichiometry is well correlated with trends in phosphate oxygen isotopic exchange
- Phosphate oxygen isotope ratios identify terrestrial P input and organic P remineralization as major P sources
- Regenerated P may support primary productivity in the deeper euphotic zone

Supporting Information:
- Supporting Information S1

Correspondence to:
D. Jaisi,
jaisi@udel.edu

Citation:
Li, J., Y. Bai, K. Bear, S. Joshi, and D. Jaisi (2017), Phosphorus availability and turnover in the Chesapeake Bay: Insights from nutrient stoichiometry and phosphate oxygen isotope ratios, *J. Geophys. Res. Biogeosci., 122*, doi:10.1002/2016JG003589.

Received 13 AUG 2016
Accepted 6 MAR 2017
Accepted article online 8 MAR 2017

Phosphorus availability and turnover in the Chesapeake Bay: Insights from nutrient stoichiometry and phosphate oxygen isotope ratios

Jiying Li[1], Yuge Bai[1], Kristi Bear[1], Sunendra Joshi[1], and Deb Jaisi[1]

[1]Department of Plant and Soil Sciences, University of Delaware, Newark, Delaware, USA

Abstract Understanding phosphorus (P) availability and its control on eutrophication in the Chesapeake Bay is complicated by variable sources and biogeochemical reactions transforming P forms. We investigated seasonal and spatial variability in P limitation and biological utilization in the Bay using nutrient stoichiometry (of both dissolved and particulate forms), phosphate oxygen isotope ratios, and alkaline phosphatase activity at three sites along the salinity gradient. We demonstrate that particulate nutrient ratios can be used as indicators of nutrient limitation in the Bay and suggest strong seasonal and spatial variability in P availability: the surface water is P limiting in spring, but this condition is alleviated in summer and in the deeper waters. Variability in P limitation is well reflected in the trends of phosphate oxygen isotope composition ($\delta^{18}O_P$), with values approaching isotopic equilibrium under P limiting conditions, suggesting rapid biological P turnover. Furthermore $\delta^{18}O_P$ values suggest multiple phosphate sources including remobilization of terrestrial inorganic P phases and remineralization of organic P and P from both sources is sufficiently cycled by microorganisms, suggested by the extensive equilibrium oxygen isotope exchange. Our results further suggest high P utilization in the deeper euphotic zone where nutrients are abundant, raising caution on studying nutrient availability and limitation only in the surface water.

1. Introduction

Chesapeake Bay, the largest estuary in the United States, is one of the most productive aquatic systems in the world. It has, however, been suffering from eutrophication and summer hypoxia since the 1950s [*Hagy et al.*, 2004; *Kemp et al.*, 2005]. Efforts toward controlling eutrophication in the Bay rely strongly on identifying the sources of phosphorus (P), one of the key limiting nutrients [*Fisher et al.*, 1992, 1999], and understanding its internal cycling and bioavailability that are temporally and spatially variable [*Ator and Denver*, 2015; *Boynton et al.*, 1995; *Kemp et al.*, 2005]. A number of studies have aimed to address seasonal and regional variations in nutrient limitation in the Bay [*Fisher et al.*, 1992, 1999; *Malone et al.*, 1996; *Prasad et al.*, 2010], using the ratios of dissolved inorganic nitrogen to dissolved inorganic phosphorus (DIN:DIP). These studies suggested P limitation in spring and N limitation in summer and early autumn [*Fisher et al.*, 1999; *Malone et al.*, 1996; *Prasad et al.*, 2010]. While deviations from the Redfield ratio (C:N:P = 106:16:1) [*Redfield*, 1958] in dissolved nutrient pools have been interpreted as evidence of nutrient limitation in aquatic systems [*Fisher et al.*, 1992; *North et al.*, 2007], the optimal N:P stoichiometry of phytoplankton (under nutrient-replete growth conditions) in the Chesapeake Bay is not known and may be different from the Redfield ratio [*Geider and La Roche*, 2002]. Moreover, whether and how DIN:DIP ratios and/or concentrations of individual nutrients regulate phytoplankton growth have long been discussed [*Downing et al.*, 2001; *Glibert et al.*, 2011; *Reynolds*, 1999], but more direct observation is lacking for the relationships between nutrient ratios, P concentrations, and biological P utilization that is coupled to primary productivity in the Bay. In this study we investigate P availability, limitation, and their seasonal and spatial variability in the water column of the Chesapeake Bay using ratios of dissolved nutrients (DIN:DIP), particulate C:N:P (PC:PN:PP), and alkaline phosphatase activity. Phosphate oxygen isotope ratios were also analyzed to identify P sources and understand P cycling in the Bay.

Phosphate (PO_4) oxygen isotope ratios ($\delta^{18}O_P$) have been applied as a tool to investigate P cycling (P sources and biological transformations) in aquatic environments [*Colman et al.*, 2005; *Elsbury et al.*, 2009; *Goldhammer et al.*, 2011; *Gooddy et al.*, 2016; *Jaisi and Blake*, 2014; *McLaughlin et al.*, 2006a, 2013; *Paytan and McLaughlin*, 2011; *Paytan et al.*, 2002; *Young et al.*, 2009]. The strong bonding between atoms of oxygen and phosphorus (P–O bond) in phosphate prevent oxygen exchange under most environmentally relevant conditions (Earth surface pressure, temperature (<80°C) and pH) [*Jaisi and Blake*, 2014; *Lécuyer et al.*, 1996]. Therefore, a

negligible isotopic effect is expected for abiotic processes such as sorption, desorption, precipitation, and transport [*Jaisi et al.*, 2010, 2011; *Liang and Blake*, 2007], which allows tracking of P sources [*Elsbury et al.*, 2009; *Gooddy et al.*, 2016; *McLaughlin et al.*, 2006a; *Young et al.*, 2009]. On the other hand, biological processes that involve P–O bond cleavage and formation/rebuilding are typically associated with large isotopic fractionations [*Blake et al.*, 2005; *Liang and Blake*, 2006a, 2006b; *Liang and Blake*, 2009]. One of the most important processes is the reversible reaction between orthophosphate and pyrophosphate catalyzed by pyrophosphatase, which exchanges all O atoms in PO_4 with ambient water O, resulting in a temperature dependent equilibrium fractionation [*Blake et al.*, 2005; *Longinelli and Nuti*, 1973]. This isotopic equilibration between PO_4 and water has been observed in many environments as an indicator of biological P turnover (i.e., PO_4 uptake, intracellular cycling, and PO_4 release into environment) [*Kolodny et al.*, 1983; *McLaughlin et al.*, 2006c, 2013; *Paytan et al.*, 2002]. Moreover, many extracellular enzymes catalyze reactions that involve breaking of P bonds and cause kinetic isotopic effects [*Blake et al.*, 1997; *Colman et al.*, 2005; *Liang and Blake*, 2009], providing a potential means to identify P sources and transformations. For example, hydrolysis of organic phosphorus involves incorporation of nucleophilic oxygen from a water molecule and generates lighter PO_4 that is indicative of PO_4 regenerated from organic P [*Colman et al.*, 2005; *Joshi et al.*, 2015; *McLaughlin et al.*, 2006b]. Here we will use phosphate oxygen isotope ratios to identify P sources, both external and internal, and their contributions to P availability. We further demonstrate that phosphate oxygen isotope ratios are indicative of P limitation in the water column of the Chesapeake Bay, linking P bioavailability to biological P utilization and turnover (i.e., P uptake, intracellular cycling, and P release).

2. Materials and Methods

2.1. Sampling Sites

Water column samples were taken at three locations across the main stem of the Chesapeake Bay in multiple seasons aboard the R/V *Kerhin* in 2014–2015 (Figure 1 and Table 1). The north site 1.1 is located at the mouth of the Susquehanna River (39.54667°N, longitude −76.08167°W); sites 3.3C and 5.2 are located at the mid Bay in the region of highest productivity (3.3C: latitude 38.99583°N, longitude −76.36000°W; 5.2: latitude 38.13667°N, longitude −76.22917°W). Site CB3.3C has been experiencing the most intense eutrophication and longest summer hypoxia of these three sites [*Zhang et al.*, 2006]. The sampling sites are the same as those of the Tidal Mainstem Water Quality Monitoring Project conducted by the Chesapeake Bay Program (CBP), where water quality data are available since 1984 (Chesapeake Bay Program, 2016, Retrieved from http://www.chesapeakebay.net/ (assessed: April 2, 2016)). The site identifications are adopted from the CBP database (CBP Water Quality Database: http://www.chesapeakebay.net/data/downloads/cbp_water_quality_database_1984_present).

2.2. Sample Collection and Nutrient Analyses

Water temperature, dissolved oxygen (DO), and salinity were measured in situ (by CBP) using a Hydrolab probe. All water samples were collected using a sampling pump and analyzed by the CBP for total particulate nitrogen (PN), particulate carbon (PC), particulate phosphorus (PP), dissolved inorganic phosphorus (DIP), nitrate and nitrite, ammonium, and concentrations of chlorophyll a and pheophytin (for details of the methods see *Chesapeake Bay Program* (CBP, 2012)). To perform isotopic analyses of water and dissolved phosphate, we collected additional water samples with volume of ~24–40 L (to attain > 5 μmol DIP) from selected depths using sampling pump (Table 1): surface (S; 0.5 m), above pycnocline (AP), below pycnocline (BP), above bottom (AB; 4–5 m above the sediment-water interface), and bottom (B; 0.5 m above the sediment-water interface). Samples were stored in coolers immediately after collection and processed upon arrival at our laboratory at the University of Delaware. Suspended particulates were separated from the water samples using centrifugation (for > 0.10 μm particles; Sorvall LYNX 6000). The separation of water and particles was completed within 2 days. Phosphate oxygen isotope analyses were conducted on the collected supernatant, following a series of concentration and purification steps (see below).

2.3. Alkaline Phosphatase Activity

Alkaline phosphatase (APase) activity was measured following a modified method of *Adams et al.* [2008]. Samples were filtered using WHATMAN 0.2 μm filters and the filtrates were incubated at 37°C at pH 8.5 (Tris-HCl buffer) using *p* nitrophenyl phosphate (*p*-NPP) as a substrate. The concentration of the produced

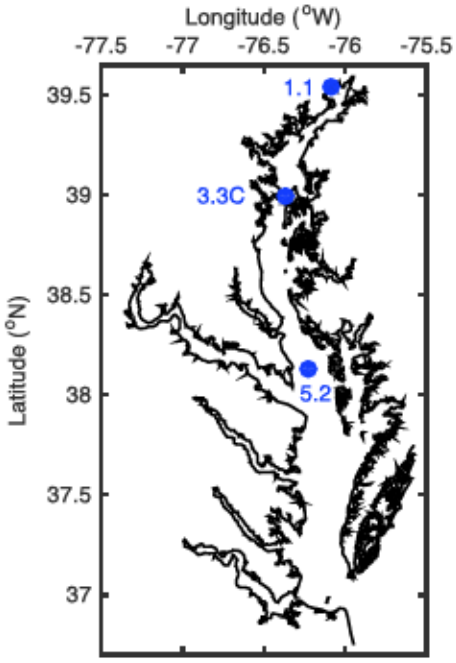

Figure 1. Sampling sites in the Chesapeake Bay.

p nitrophenol (*p*-NP) was measured by spectrophotometer at 410 nm. APase activity was calculated as μmol *p*-NPP hydrolyzed (*p*-NP or PO_4 produced) per hour per liter of water. To account for the differences in biomass among samples, APase activities (μmol P h^{-1} L^{-1}) were also divided by total suspended solid (TSS) (Table S1 to S3 in the supporting information) for comparison.

2.4. Phosphate and Water Oxygen Isotope Analyses

To analyze phosphate oxygen isotope ratios ($\delta^{18}O_P$) in the DIP pool, DIP in water samples was concentrated using the magnesium-induced coprecipitation (MagIC) method [*Karl and Tien*, 1992; *Thomson-Bulldis and Karl*, 1998], followed by treatment with Superlite™ DAX-8 resin and cation exchange resin (Bio-Rad AG50W-X8) to remove impurities [*Gross et al.*, 2013; *Joshi et al.*, 2015; *Tamburini et al.*, 2010]. Samples were further purified using sequential precipitation and recrystallization methods [*Kolodny et al.*, 1983; *O'Neil et al.*, 1994], purified with cation exchange resin, and finally converted to silver phosphate prior to analyses for oxygen isotope composition. Oxygen isotope compositions of silver phosphate samples were analyzed using a Thermo Chemical Elemental Analyzer (TC/EA) coupled with a Delta V continuous flow isotope ratio mass spectrometer (IRMS; Thermo-Finnigan, Bremen, Germany): oxygen in Ag_3PO_4 was liberated by decomposition at 1460°C to react with glassy carbon to form CO for determination of $^{18}O/^{16}O$ ratios. The $\delta^{18}O_P$ values were calibrated against conventionally fluorinated two Ag_3PO_4 standards, YR 3-2 (33.63‰) and YR 1-1aR 02 (−5.45‰). Three replicate Ag_3PO_4 samples were measured for each sample and standard; one standard deviation of the mean is reported as uncertainty. Typical precision for replicate standards was 0.1–0.3‰. For Ag_3PO_4 samples without replicates due to sample amount limitation, precision 0.3‰ was used as uncertainty.

Measurements of water oxygen isotopic compositions ($\delta^{18}O_w$) were conducted using a Finnigan™ GasBench II coupled with IRMS: a small amount of CO_2 in the headspace of the sample vials was introduced into IRMS and measured for $^{18}O/^{16}O$ ratios after complete equilibrium with the sample at 26°C (>24). The $\delta^{18}O_w$ values were calibrated against two U.S. Geological Survey (USGS) standards: W67400 (−1.97‰) and USGS W32615 (−9.25‰). Duplicate water samples and triplicate standards were analyzed, and one standard deviation of the mean is reported as uncertainty. Typical precision for replicate standards was <0.06‰. $\delta^{18}O_P$ and $\delta^{18}O_w$ values are reported following standard delta notation relative to Vienna Standard Mean Ocean Water.

2.5. Calculation of Isotopic Equilibrium Values for Phosphate

The theoretical isotopic equilibrium values ($\delta^{18}O_{Eq}$; expected for full biological P turnover of phosphate and wholesale exchange of oxygen between phosphate and ambient water [*Blake et al.*, 1998, 2005]) can be determined using phosphate-water fractionation equations. In this study we used two most commonly used equations, i) derived from observed O-isotope fractionations between phosphate (PO_4) and water in biogenic phosphate minerals [*Longinelli and Nuti*, 1973]:

$$T\,(℃) = 111.4 - 4.3\left(\delta^{18}O_{Eq} - \delta^{18}O_w\right) \quad (1)$$

and ii) newly determined equation for equilibrium O-isotope fractionations between dissolved phosphate and water (fractionation factor $\alpha(PO_4 - H_2O)$) [*Chang and Blake*, 2015]:

Table 1. Oxygen Isotopic Compositions of Water ($\delta^{18}O_w$), Dissolved Phosphate ($\delta^{18}O_P$), and Calculated Equilibrium Phosphate Oxygen Isotopic Compositions ($\delta^{18}O_{Eq.1}$ Was Calculated Following *Chang and Blake* [2015] and $\delta^{18}O_{Eq.2}$ Was Calculated Following *Longinelli and Nuti* [1973] From Different Sites, Seasons, and Water Depths in the Chesapeake Bay.)[a]

Site	Time	Layer	Depth (m)	T (°C)	$\delta^{18}O_w$ (‰)	$\delta^{18}O_P$ (‰)	$\delta^{18}O_{Eq.1}$ (‰)	$\delta^{18}O_{Eq.2}$ (‰)
1.1	3/20/2014	S	0.5	4.5	−10.24 ± 0.10	15.10 ± 0.12	15.28	14.62
		B	6	4.5	−10.14 ± 0.09	15.28 ± 0.16	15.38	14.72
1.1	5/14/2014	S	0.5	19.5	−9.06 ± 0.01	17.78 ± 0.37	13.79	12.31
		B	6	19.4	−9.09 ± 0.04	/	13.77	12.32
1.1	7/9/2014	S	0.5	28.2	−8.01 ± 0.01	/	13.42	11.34
		B	4	27.8	−8.03 ± 0.04	17.23 ± 0.85	13.46	11.41
1.1	9/17/2014	S	0.5	23.9	−7.70 ± 0.03	25.51 ± 0.13	14.44	12.65
		B	4	23.4	−7.75 ± 0.02	22.78 ± 0.82	14.47	12.72
1.1	5/7/2015	S	0.5	18.9	−9.59 ± 0.02	16.73 ± 0.36	13.35	11.92
		B	5	19.7	−9.43 ± 0.01	17.58 ± 0.15	13.37	11.89
3.3C	3/19/2014	S	0.5	3.5	−6.66 ± 0.01	19.23 ± 0.06	19.15	18.43
		BP	18	3.1	−4.03 ± 0.01	20.58 ± 0.37	21.92	21.16
		B	24	3.1	−4.45 ± 0.01	18.09 ± 0.36	21.49	20.73
3.3C	5/13/2014	S	0.5	20.9	−7.47 ± 0.02	15.49 ± 0.10	15.17	13.58
		BP	13	11.5	−4.42 ± 0.03	19.73 ± 0.71	19.95	18.81
		B	23	11.4	−4.12 ± 0.03	18.85 ± 0.46	20.27	19.14
3.3C	7/8/2014	S	0.5	25.8	−6.00 ± 0.10	18.05 ± 0.06	15.86	13.91
		BP	17	22.0	−4.64 ± 0.02	17.90 ± 0.20	17.88	16.15
		B	24	21.6	−4.33 ± 0.05	17.30 ± 0.62	18.27	16.55
3.3C	9/16/2014	S	0.5	23.5	−4.31 ± 0.09	21.30 ± 0.34	17.97	16.13
		BP	14	25	−3.41 ± 0.02	18.85 ± 0.37	18.64	16.68
		B	23	25.2	−3.30 ± 0.02	19.16 ± 0.49	18.78	16.75
3.3C	5/6/2015	S	0.5	17.8	−7.03 ± 0.12	13.29 ± 0.26	16.16	14.74
		BP	16	10.5	−4.75 ± 0.05	17.12 ± 0.35	19.78	18.71
		B	24	10.3	−4.20 ± 0.09	18.75 ± 0.28	20.40	19.32
3.3C	7/7/2015	S	0.5	27.3	−6.23 ± 0.08	14.78 ± 0.18	15.38	13.33
		AP	4	25.9	−6.13 ± 0.03	/	15.71	13.75
		BP	13	22.8	−4.29 ± 0.11	17.54 ± 0.20	18.10	16.31
		AB	21	22.4	−3.96 ± 0.01	17.80 ± 0.90	18.51	16.73
		B	24	22.4	−3.72 ± 0.02	19.16 ± 0.39	18.79	17.02
3.3C	9/15/2015	S	0.5	24.3	−4.60 ± 0.09	18.29 ± 0.26	17.54	15.66
		AP	4	24.3	−4.45 ± 0.06	17.37 ± 0.07	17.69	15.80
		BP	12	26.1	−3.22 ± 0.08	18.25 ± 0.09	18.65	16.62
		AB	19	26.1	−3.06 ± 0.07	18.78 ± 0.39	18.82	16.78
		B	23	26.1	−3.03 ± 0.04	18.33 ± 0.13	18.85	18.81
5.2	3/19/2014	S	0.5	3.3	−3.93 ± 0.04	/	21.99	21.21
		BP	21	3.9	−3.68 ± 0.01	21.37 ± 0.22	22.13	22.32
		B	31	4.0	−3.47 ± 0.01	18.66 ± 0.20	22.32	22.51
5.2	5/12/2014	S	0.5	17.8	−5.90 ± 0.04	19.00 ± 0.38	17.31	15.87
		BP	15	13.7	−3.11 ± 0.03	20.82 ± 0.84	20.89	19.61
		B	30	13.3	−2.73 ± 0.01	21.48 ± 0.06	21.35	20.08
5.2	7/7/2014	S	0.5	25.4	−4.43 ± 0.05	15.99 ± 0.31	17.53	15.57
		BP	22	24.3	−3.74 ± 0.05	18.40 ± 0.26	18.42	16.51
		B	29	24.1	−3.48 ± 0.01	18.17 ± 0.50	18.72	16.82
5.2	9/15/2014	S	0.5	24.4	−3.67 ± 0.02	21.77 ± 0.55	18.47	16.56
		BP	19	24.9	−3.20 ± 0.11	23.79 ± 0.44	18.87	16.92
		B	29	25.3	−2.94 ± 0.05	19.61 ± 0.34	19.07	17.08
5.2	5/5/2015	S	0.5	16.2	−5.58 ± 0.02	16.85 ± 0.26	17.92	16.56
		BP	13	13.6	−2.98 ± 0.05	20.52 ± 0.25	21.04	19.76
		B	30	13.2	−2.72 ± 0.01	20.82 ± 0.22	21.38	20.12

[a]S, surface, 0.5 m; AP, above pycnocline; BP, below pycnocline; AB, above bottom, 4–5 m above the sediment-water interface; and B, bottom, 0.5 m above the sediment-water interface.

$$1000 \ln a(PO_4 - H_2O) = 14.43 \times 1000/T(K) - 26.54 \quad (2)$$

or

$$\delta^{18}O_{Eq} = \left(\delta^{18}O_w + 1000\right) \times e^{\left[14.43\,x\,(1000/T) - 26.54\right]/1000} - 1000 \quad (3)$$

Please note *T* in equation (1) represents temperature in degree *Celsius* (°C) but in equations (2) and (3) it is in degree kelvin (K). Expected equilibrium values for phosphate oxygen isotope ratios were calculated for each sample using the measured water oxygen isotope ratios (see section 2.4) and measured temperature.

3. Results

3.1. Dissolved Oxygen, Nitrogen, and Phosphorus

The water column of the Chesapeake Bay exhibited strong spatial and seasonal variability in concentrations of dissolved oxygen, and concentrations of inorganic nitrogen and phosphorus (Figure 2). At site 1.1, concentrations of nitrate and nitrite (referred as nitrate (NO_3^-) hereafter for simplicity) were high (~09–75 μmol L^{-1}) for all seasons, while DIP concentrations were much lower (<1 μmol L^{-1}) (Figure 2). At sites 3.3C and 5.2, nitrate concentrations in the surface water decreased from March to September (e.g., from 68 μmol L^{-1} to < 2 μmol L^{-1} at site 3.3C; Figure 2). Nitrate also decreased with depth and was nearly depleted in the anoxic waters in July and September (Figure 2). In contrast, ammonium concentrations increased with depth, and the concentrations in bottom waters increased throughout the summer with the highest concentration in July (Figure 2). DIP concentrations were low for the entire water column in the well-oxygenated seasons (March–May), but concentrations increased in deeper anoxic waters in the hypoxic/anoxic seasons (May–September; Figure 2). The strong seasonality in the Chesapeake Bay water column is also illustrated in Figures 3a-1, 3b-1, and 3c-1, which show the variability in surface temperature, productivity (as indicated by pigment concentrations), and concentrations of NH_4^+ and DIP.

3.2. The Ratios of Dissolved and Particulate C:N:P

The ratios of dissolved nutrients (DIN:DIP), particulate carbon to nitrogen (PC:PN), particulate carbon to phosphorus (PC:PP), and particulate nitrogen to phosphorus (PN:PP) are complied and shown in Figure 3. At site 1.1, the high NO_3^- and low DIP concentrations (Figure 2) resulted in larger DIN:DIP (values generally > 100) compared to the Redfield ratio (Figure 3a-2). The values of PC:PP and PN:PP showed large fluctuations around the Redfield ratios (106:1P and 16PN:1PP, respectively; Figures 3a-3 and 3a-4). At sites 3.3C and 5.2, the average DIN:DIP ratio increased from winter (December) to spring (March–May), declined throughout the summer, reached a minimum in September and then recovered toward the Redfield ratio in winter (Figures 3b-2 and 3c-2). At these sites, the PC:PP and PN:PP values showed similar seasonal trends, with values increasing in spring (March–May) and decreasing in summer and fall (July–November). Both ratios generally decreased with depth, with values at the bottom closer to the Redfield ratio (Figures 3b-3, 3b-4, 3c-3, and 3c-4).

3.3. Alkaline Phosphatase Activity

The APase activities at both sites 3.3C and 5.2 were generally high in May (average 0.30 and 0.80 μmol P h^{-1} L^{-1}, respectively) compared to July and September (at site 3.3C average 0.07 and 0.05 μmol P h^{-1} L^{-1}, respectively; at site 5.2 near detection limit (0.01 μmol P h^{-1} L^{-1})) (Figure 4). At sites 3.3C and 5.2, APase activities generally decreased with depth (e.g., from 0.30 μmol P h^{-1} L^{-1} in surface waters to undetectable in bottom waters in May 2014). At site 1.1, however, no clear trend was observed.

3.4. Oxygen Isotopic Compositions of Water and Dissolved Phosphate

Water oxygen isotope compositions ($\delta^{18}O_w$) in the water column of the Chesapeake Bay varied spatially and seasonally (Table 1 and Figure 5), with $\delta^{18}O_w$ values ranging from −7.70 to −10.24‰ at the freshwater site 1.1 and from −2.72 to −4.43‰ at the most saline site 5.2. The $\delta^{18}O_w$ values at sites 3.3C and 5.2 were linearly correlated to salinity (Figure 5a), representing typical conservative mixing behavior: least squares linear relationship $\delta^{18}O_w$ (‰) = 0. 249× Salinity − 8.01 for site 3.3C (r^2 = 0.907) and $\delta^{18}O_w$ (‰) = 0. 242× Salinity − 7.90 for site 5.2 (r^2 = 0.931) with salinity expressed in practical salinity unit (psu). The $\delta^{18}O_w$ values at the fresh water site 1.1 (salinity = 0 psu), however, also exhibited a large spread corresponding to seasonality, increasing from spring (March) to late summer (September) and then decreasing in fall (Figure 5b).

Oxygen isotopic compositions of dissolved phosphate ($\delta^{18}O_P$) and the calculated theoretical equilibrium values ($\delta^{18}O_{Eq}$) are shown in Table 1; their depth distributions and seasonal trends are presented in Figures 6 and 7, respectively. The equilibrium values ($\delta^{18}O_{Eq}$) were lightest at the freshwater site 1.1, and generally became heavier with increasing salinity toward the ocean and deeper waters (saline water intruded from the ocean via bottom currents; Figure 6). At site 1.1, $\delta^{18}O_P$ values gradually became heavier from March

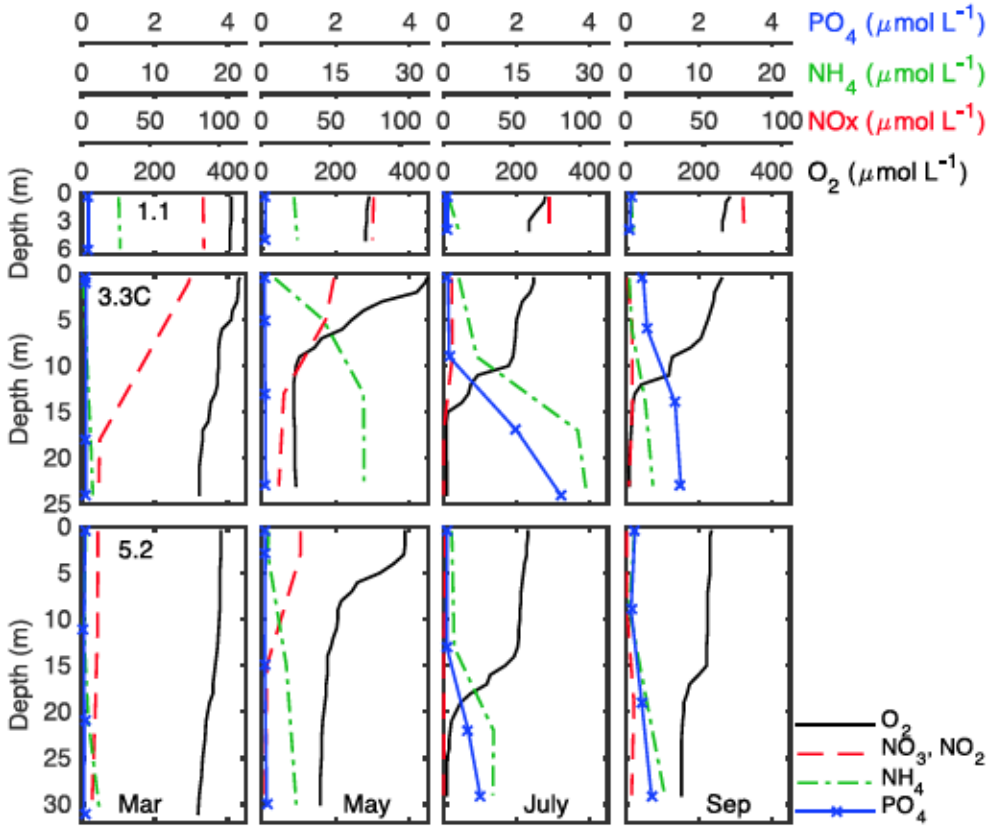

Figure 2. Vertical distributions of temperature (°C), salinity (psu), concentrations of chlorophyll *a* and pheophytin (μg L^{-1}), dissolved O_2 (mg L^{-1}), nitrate + nitrite (NO_x; Mmol L^{-1}), ammonium (NH_4^+; Mmol L^{-1}), and phosphate (PO_4; Mmol L^{-1}) in the water column of the Chesapeake Bay in different seasons (March, May, July, and September) in 2014 (distributions in 2015 were similar). The upper, middle, and lower panels are from sites 1.1, 3.3C and 5.2, respectively.

to September, and trending away from equilibrium values (Figure 6). At sites 3.3C and 5.2, $\delta^{18}O_P$ values seem to generally follow the trend of equilibrium values (Figure 6), with exceptions in the surface waters for 2014 samples in which $\delta^{18}O_P$ values became considerably heavier than $\delta^{18}O_{Eq}$ in hypoxic/anoxic seasons (July, September; Figures 5 and 6). The $\delta^{18}O_P$ values in the bottom waters showed less seasonal variability and were generally close to or slightly lighter than $\delta^{18}O_{Eq}$ (Figure 7). In March and September months, the $\delta^{18}O_P$ values showed higher offset than the calculated $\delta^{18}O_{Eq}$ values than in other seasons (Figure 7).

4. Discussion

4.1. Phosphorus Availability and Nutrient Stoichiometry

The strong seasonality in redox stratification in the water column of the Chesapeake Bay has led to spatial and temporal variability in P availability and nutrient stoichiometry. The consistently high DIN:DIP ratios (compared to Redfield ratios) at site 1.1 suggest P limitation conditions throughout the entire year, whereas at sites 3.3C and 5.2, seasonal variations in DIN:DIP ratios suggest changing nutrient limitation status (Figure 3). The variations in P availability and thus biological P stress (P limitation for biological activities such as growth of phytoplankton and other microorganisms) were also reflected in the spatial and seasonal variations in PC:PP and PN:PP ratios (Figure 3). The effect of P availability (DIP concentrations) on the ratios of particulate (consisting of biomass) C, N, and P can be demonstrated in Figure 8: both PC:PP and PN:PP values markedly increased when DIP concentrations decreased to a tipping point at ~0.2–0.5 μmol L^{-1} and reached a maximum of ~250–450 for PC:PP and ~30–60 for PN:PP. This is likely because changes in nutrient availability and stoichiometry fundamentally affect food quality thus the makeup of primary producer communities [*Sterner and Elser*, 2002; *Suttle and Harrison*, 1988].

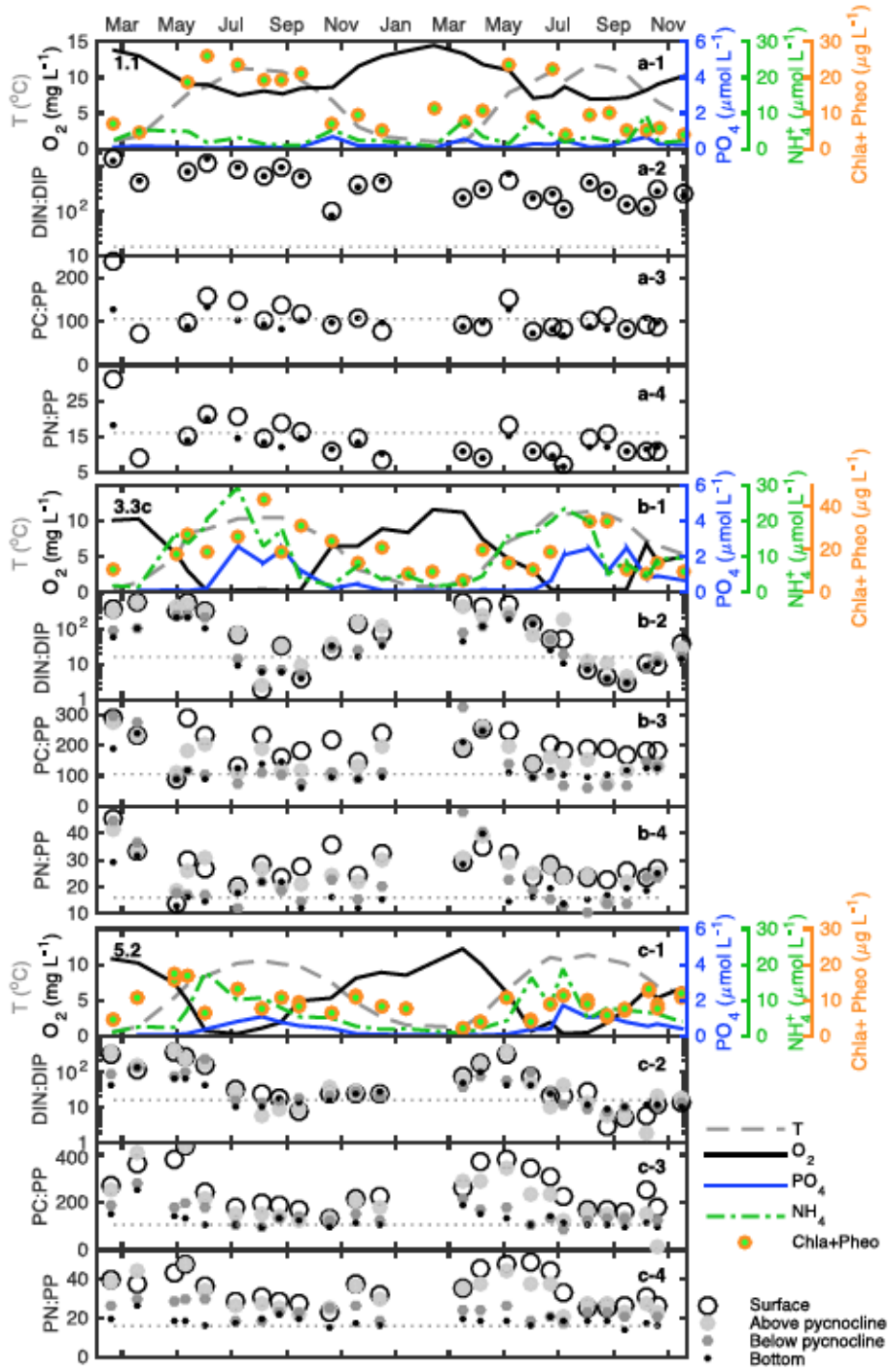

Figure 3. Seasonal variations of surface temperature (°C), chlorophyll *a* and pheophytin (μg L^{-1}) in the surface waters, dissolved O_2 (mg L^{-1}), ammonium (μmol L^{-1}), and phosphate (μmol L^{-1}) in the bottom waters, and the ratios of DIN:DIP, PC:PN, PC:PP, and PN:PP in the water column at sites (a1–a4) 1.1, (b1–b4) 3.3C, and (c1–c4) 5.2.

The high DIN:DIP, PC:PP, and PN:PP ratios (above Redfield) during spring to summer (March and May) at sites 3.3C and 5.2 (Figures 3b and 3c) may be indicative of P limitation in spring to early summer. This is due to the low DIP concentrations and rapid increase of phytoplankton biomass in the spring with increasing temperature (Figures 1 and 2). During summer stratification and development of bottom water hypoxia (Figure 2), these ratios markedly decreased (e.g., at 5.2 DIN:DIP, PC:PP, and PN:PP were close to Redfield ratio; Figures 3c-2–3c-4) due to the excess supply of DIP from the hypoxic/anoxic deeper waters (Figure 2). The

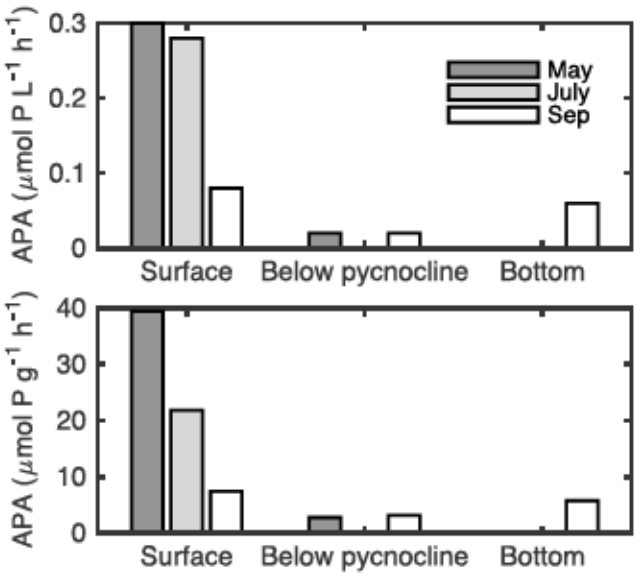

Figure 4. Activity of alkaline phosphatase (APase) at site 3.3C (2014). APA at Below pycnocline in July and bottom in May and July were lower than detection limit (0.01 μmol P L^{-1} h^{-1}). The APase activity was measured in μmol P L^{-1} h^{-1} and also calculated as μmol P g^{-1} h^{-1} using TSS (mg/L; see Table S2).

supply of DIP (through P remobilization/remineralization; see discussion in the following sections) led to less P stress, which may explain the decrease of PC:PP and PN:PP ratios with depth (Figure 3). Preferential degradation of P compared to C and reductive dissolution of Fe-P, as suggested in some anoxic environments [*Jilbert et al.*, 2011], would have increased the PC:PP and PN:PP values with depth if occurring in the Bay, and thus, is unlikely to explain the vertical trends. Sorption of DIP onto particles is also unlikely to have contributed to the trends: loosely sorbed P in the particles in the water column of the bay was determined to be <10% of total particulate P, and no vertically decreasing trend of this pool was observed (data not shown). Therefore, the vertical changes of PC:PP and PN:PP ratios were likely due to increasing P concentrations and changing stoichiometry in biomass synthesis.

Interpretation of nutrient stoichiometry (i.e., DIN:DIP and PN:PP) as indicators for nutrient limitation may be challenged by several uncertainties. First, instead of strictly following the Redfield ratio (16N:1P), optimal N:P stoichiometry of phytoplankton (under nutrient-replete growth conditions) may vary (from 5 to 19, with most observations below the Redfield ratio number of 16 [*Geider and La Roche*, 2002]), depending on ecological conditions [*Klausmeier et al.*, 2004]. The critical N:P ratio that marks the transition between N and P

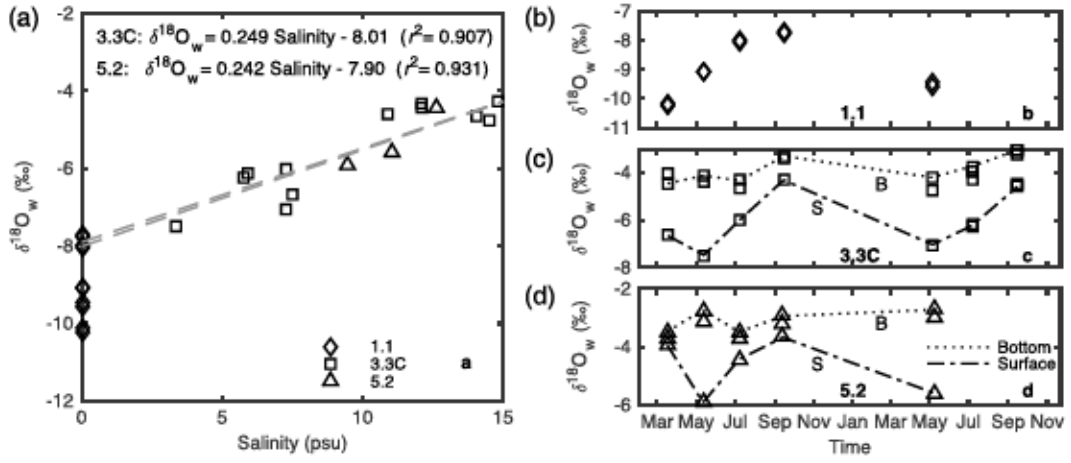

Figure 5. Relationship of water oxygen isotopic composition ($\delta^{18}O_w$) with salinity (dashed lines are the linear fit to the data) (a), and seasonal variations of water oxygen isotopic composition at sites (b) 1.1, (c) 3.3C, and (d) 5.2.

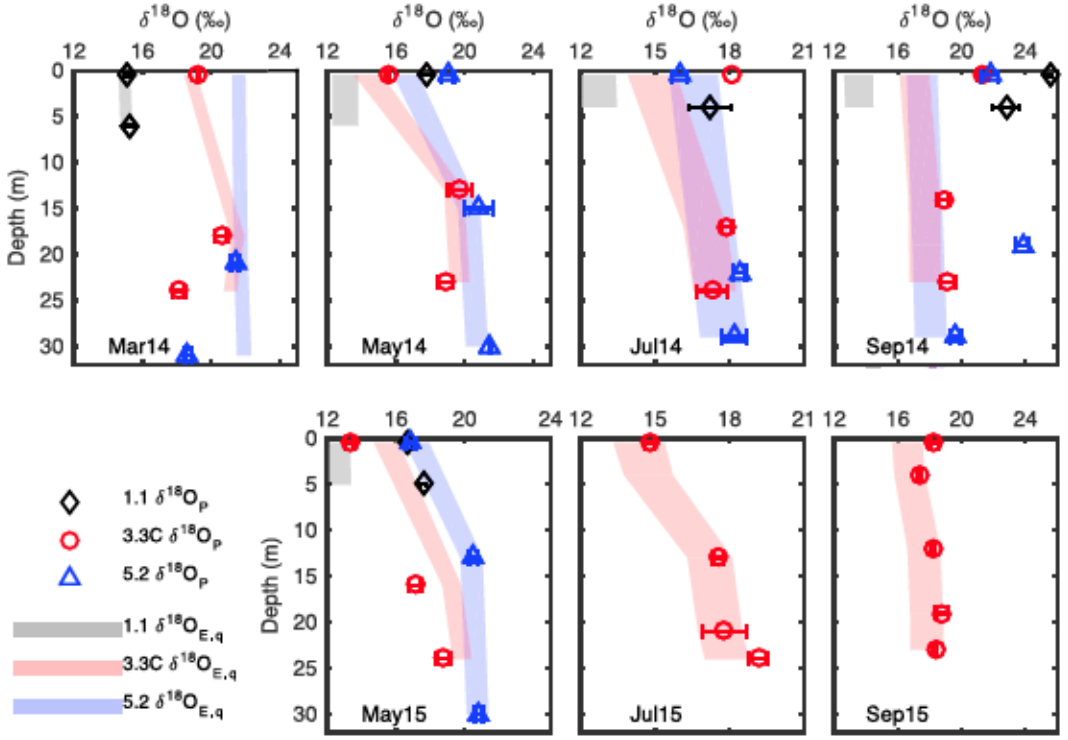

Figure 6. Vertical distributions of oxygen isotopic compositions of dissolved phosphate ($\delta^{18}O_P$ (‰); symbols) and calculated theoretical equilibrium values ($\delta^{18}O_{Eq.}$ (‰); shaded zones) in the water column of the Chesapeake Bay. The theoretical isotopic equilibrium values were calculated using the equation for equilibrium O-isotope fractionation between dissolved phosphate and water, with the upper limit of the shaded zone calculated using *Chang and Blake* [2015] and the lower limit calculated using *Longinelli and Nuti* [1973]. The top and bottom panels include data from 2014 and 2015, respectively.

limitation likely lies in the range of 15–30 for algae and cyanobacteria [*Geider and La Roche*, 2002]. The optimal N:P stoichiometry of phytoplankton and the critical N:P ratio for nutrient limitation in the Chesapeake Bay is not known; however, relationships of PC:PN:PP and nutrient concentrations suggest that the optimal stoichiometry is close to the Redfield ratio: the PC:PN:PP values approach Redfield ratios when concentrations increase (Figure 8). Second, the PC:PN:PP ratios may not be representative of that of the phytoplankton C:N:P, as the particles may consist of inorganic fractions, especially inorganic phosphorus fractions such as iron

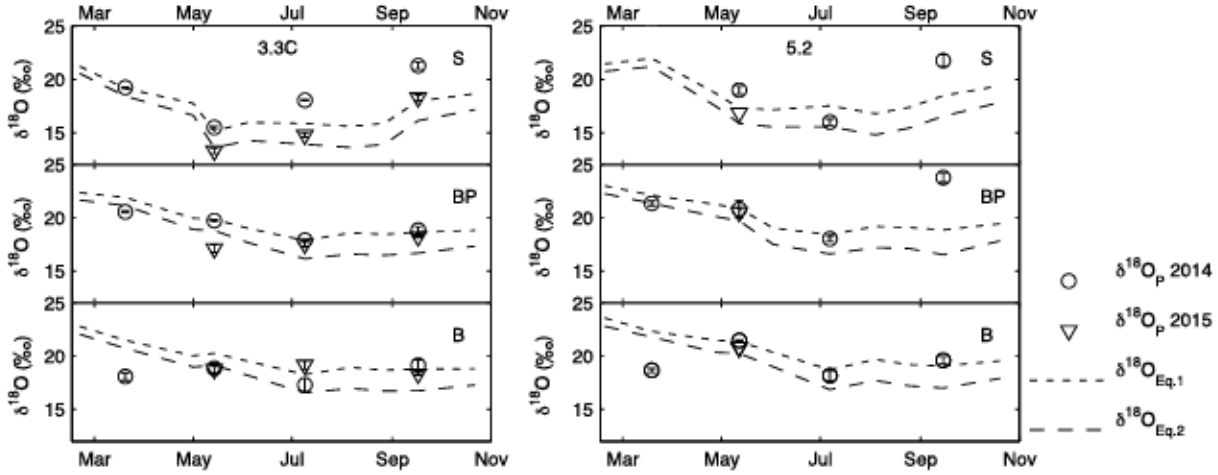

Figure 7. Seasonal variations of oxygen isotopic compositions of dissolved phosphate ($\delta^{18}O_P$ (‰); symbols) and calculated theoretical equilibrium values ($\delta^{18}O_{Eq.}$ (‰); dashed [*Longinelli and Nuti*, 1973] and dotted lines [*Chang and Blake*, 2015]) at sites (left column) 3.3C and (right column) 5.2. Where $\delta^{18}O_w$ were not measured, $\delta^{18}O_{Eq}$ was calculated using $\delta^{18}O_w$ calculated using the linear relationship between $\delta^{18}O_w$ and salinity (see Figure 5).

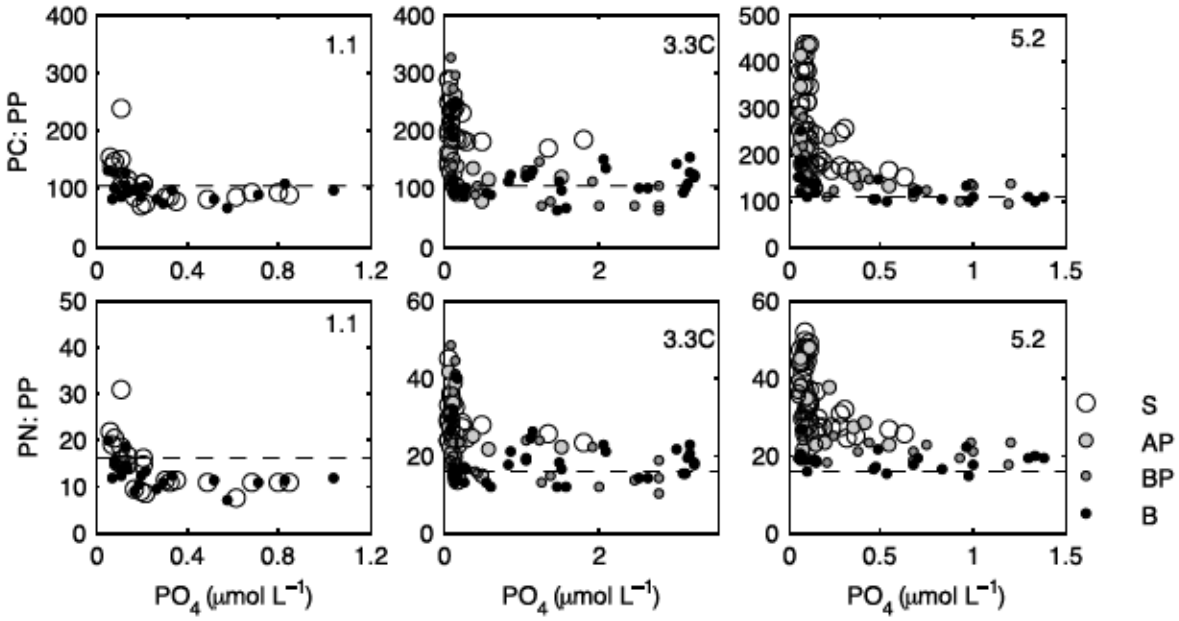

Figure 8. Correlations of particulate C:N:P stoichiometry vs. concentrations of dissolved nitrogen and phosphorus.

hydro(oxide) bound P (Fe-P). At site 1.1, with more input of allochthonous inorganic P (>10% and in some cases ~50%; e.g., coming from the Susquehanna River [*Biggs*, 1970; *Hartzell*, 2009; *Keefe*, 1994]), the PC:PN:PP values are likely underestimated. In the middle Bay (i.e., sites 3.3C and 5.2) where primary productivity is high and fluvial input is less important, particulates comprise largely organic P especially in the surface water [*Keefe*, 1994], with inorganic P accounting for ~20–30% of the total particulate P [*Keefe*, 1994]. The PC:PN:PP ratios therefore likely underestimate the biomass C:N:P ratios by ~6–40%. In spite of these uncertainties, the measured activities of alkaline phosphatase, an enzyme that is produced to hydrolyze organic P compounds and release phosphate molecules when organisms are P limited [*Duhamel et al.*, 2010; *Nicholson et al.*, 2006], support the seasonal and vertical trends of P limiting conditions indicated by the nutrient ratios. APase activity decreased from May to September and decreased with depth at sites 3.3C and 5.2 in 2014 (Figure 4). However, measurements of APase activity may be subject to uncertainties due to changes in biomass and community structures. For example, APase activity appeared similar in surface water in May and July 2014 at site 3.3C (Figure 4) when measured in μmol $P\,L^{-1}\,h^{-1}$, likely due to the higher productivity although less P limiting condition in July (Figure 3b). When normalized to TSS, an estimate of biomass, APase activity in July was significantly lower (22 μmol $P\,g^{-1}\,h^{-1}$ compared to 40 μmol $P\,g^{-1}\,h^{-1}$ in May; Figure 4). Moreover, expression of APase and its response to P limitation can be species dependent [*Stout et al.*, 2014]; thus, seasonal changes in community structure could have complicated the comparison. Nevertheless, our results in APase activities and nutrient ratios (for both dissolved and solid phases) are broadly consistent. These results are also largely consistent with bioassay studies conducted in the surface waters of the Bay that are indicative of seasonal shifts in nutrient limitations [*Fisher et al.*, 1999; *Kemp et al.*, 2005].

4.2. PO_4 Isotopes Identifying P Sources

Oxygen isotope compositions of dissolved phosphate are useful parameter for understanding P sources and cycling, as $\delta^{18}O_P$ values reflect various sources of DIP and biological P transformations through oxygen exchange and isotopic fractionations [*Jaisi and Blake*, 2014; *Paytan and McLaughlin*, 2011]. At site 1.1, the near equilibrium $\delta^{18}O_P$ values in March suggested rapid biological P turnover in the early spring phytoplankton bloom (see discussion in section below); however, $\delta^{18}O_P$ values continually became heavier from March to September, which may reflect source signatures. The major external sources of P to the Chesapeake Bay include river flow carrying both dissolved and particulate P, ground water seepage, point discharge, and atmospheric deposition, among which riverine input accounts for >66% of the total P input [*Boynton et al.*, 1995]. Site 1.1 is strongly influenced by terrestrial inputs and riverine inflow from the Susquehanna River [*Hartzell*, 2009] and lies in the estuarine turbidity maximum zone. Particulate P coming from land and

tributaries typically includes Fe and Al oxide-bound P and loosely sorbed P [*Conley et al.*, 1995] which may potentially release DIP into the Chesapeake Bay water [*Conley et al.*, 1995]. The phosphate oxygen isotope ratios of loosely sorbed P and Fe and Al oxide-bound P in particulates in a tributary to the Chesapeake Bay were found to be in the range of ~16–19‰ and ~19–24‰, respectively [*Bear*, 2016]. The $\delta^{18}O_P$ values for Fe and Al oxide-bound P for particulates from agricultural soils, stream banks, wetlands, manure, and forest in the East Creek (MD) in the Chesapeake Bay watershed (nearby the tributary) varied in the range of ~21–26‰ [*Bear*, 2016]. While $\delta^{18}O_P$ values of dissolved P input by rivers are not known but likely fall between the isotope values of particulate P and equilibrium $\delta^{18}O_{Eq}$ values ($\delta^{18}O_{Eq}$ ~ 17–20‰) [*Bear*, 2016]. For example, $\delta^{18}O_P$ values for river water near an agriculture field was found to be ~20–23‰ [*Bear*, 2016]. Assuming similar ranges of isotope compositions for P sources in the upper Bay, we hypothesize that the higher $\delta^{18}O_P$ values in later seasons reflect source signatures from land and riverine discharge. Interestingly, higher-than-equilibrium values were also observed for Fe oxide-bound P in the surface sediments in the Bay (e.g., 18–22‰, average ~21‰) [*Joshi*, 2016; *Joshi et al.*, 2015], further suggesting the distinct isotopic signature of the deposited particulate Fe-P that may undergo remobilization in the water and sediment columns, releasing DIP into the water column. Resuspension of sediment particles therefore may also contribute to the particulate P pool in the water column and release DIP. The terrestrial/riverine sources of dissolved and particulate P may also be important in the middle and lower Bay at sites 3.3C and 5.2, in which $\delta^{18}O_P$ values increased in the later seasons (July and September 2014, although such a trend was less apparent in 2015) (Figure 8). On the other hand, the heavier $\delta^{18}O_P$ values could have resulted from transport of water and nutrient within the mainstem Bay. However, distinguishing the local terrestrial/riverine P sources (e.g., site 5.2 is downstream of the Patuxent River and close to the Potomac River) and P from upstream surface flow is difficult given the limiting isotope data of the potential sources.

In addition to remobilization of particulate inorganic P (e.g., Fe-P) that releases DIP into the water column, remineralization of organic P and condensed inorganic P phases (called "organic P" hereafter for simplicity) is also an important source of water column DIP. This is reflected in the lighter than equilibrium $\delta^{18}O_P$ values, especially in the deeper water column (e.g., 14 March and 15 May, Figure 4), suggesting remineralization of organic P into the DIP pool [*Colman et al.*, 2005; *Joshi et al.*, 2015]. Disequilibration of isotope values (lower than equilibrium values) is expected during organic P remineralization due to large isotopic effects including (i) incorporation of lighter oxygen from water (−10.3 to −2.8‰; Figure 5 and Table 1) into the released orthophosphate and (ii) large isotope fractionations associated with P remineralization/hydrolysis catalyzed by phosphohydrolase enzymes (with enzyme and substrate specific isotopic fractionation factors range from −30 to −10‰, and could be positive (6–10‰) for the case of phytic acid hydrolysis catalyzed by phytase and acid phosphatase) [*Liang and Blake*, 2006a, 2006b; *Liang and Blake*, 2009; *Sun et al.*, 2017; *von Sperber et al.*, 2015]. On the other hand, the lighter than equilibrium values in the bottom water in early spring (March and May) could possibly reflect the lack of isotopic equilibration during the winter: it is possible that the released DIP in the deep waters during the warmer months (July–September) equilibrates with source water but retains the light isotope compositions during the darker and cooler winter months when biological activity is low. This may explain the similar $\delta^{18}O_P$ values in the bottom waters between March and the summer months July–September (Figure 7).

4.3. Biological P Turnover Indicated by PO_4 Isotope Ratios

Phosphate oxygen isotope exchange with water has been well correlated with microbial respiration and P utilization in culture experiments [*Blake et al.*, 1998; *Stout et al.*, 2014] and thus could be potentially useful to identify biological P turnover (i.e., P uptake, intracellular cycling, and release into the ambient water) and P limitation status in natural environments. In controlled laboratory experiments with an enzyme (inorganic pyrophosphatase) that catalyzed the phosphate oxygen isotopic equilibrium reaction (the reversible reaction between orthophosphate and water by pyrophosphatase), equilibrium was achieved within 24 h at 22°C and within ~ 48 h at 6°C [*Blake et al.*, 2005]. The timescale for P turnover and phosphate isotopic equilibrium in natural systems depends on growth conditions of the organisms in the system, concentrations of P (P limiting or not), and other kinetic isotope effects on the phosphate oxygen isotope values [*Blake et al.*, 2005]. The near equilibrium values of $\delta^{18}O_P$ in the surface water at sites 3.3C and 5.2 in the early seasons of the year (March–May) (Figure 5) suggest rapid P turnover, which is consistent with the low DIP and P limiting conditions as indicated by the DIN:DIP, PC:PP, and PN:PP ratios (Figures 1b and 1c; see discussion above).

The equilibrium $\delta^{18}O_P$ values also suggest that P turnover is faster compared to transport of P by water and material movements. In the Chesapeake Bay, water movement is characterized by a typical long-term gravitational circulation, consisting of lighter riverine freshwater water moving at the surface toward the ocean and oceanic (saline) water flowing in the opposite direction on the bottom (toward the head of the Bay) [*Pritchard*, 1956, 1967]. This is reflected in the large seasonal and spatial variations in water oxygen isotope values (Figure 5), and the corresponding variations in $\delta^{18}O_{Eq}$ values (Figure 7). Tidal current is also an important mixing mechanism in the Bay [*Boicourt et al.*, 1999] and the cycle period is similar to the timescale for rapid isotope equilibrium (24–48 h, see above). For a typical salinity variation of <2 psu within one tidal cycle, the effect on $\delta^{18}O_W$ and $\delta^{18}O_{Eq}$ is ~0.5‰ (based on the equations in Figure 5 and section 2.5), which is within the uncertainty range of $\delta^{18}O_P$ values measured (Table 1) and thus can be neglected. The heavier $\delta^{18}O_P$ values in the later seasons (July and September 2014) indicates the dominance of the source signatures (e.g., from remobilization of Fe-P; see discussion above), likely because of decreasing P turnover rates due to increased supply of DIP in the summer, consistent with the low PC:PP and PN:PP values and thus less/no P limitation after summer (see discussion above).

Whereas the $\delta^{18}O_P$ values in the upper layers (S and BP) showed strong seasonal variations, either following the trends of $\delta^{18}O_{Eq}$ because of rapid P turnover or reflecting source signatures, the $\delta^{18}O_P$ values in the bottom waters showed relatively less variability (Figure 7). For example in March $\delta^{18}O_P$ values in the bottom waters were similar to those in other seasons, although $\delta^{18}O_{Eq}$ were much higher. This suggests that P turnover in March is not sufficient to achieve $\delta^{18}O_P$ equilibrium in the bottom waters, which is expected because of slower growth of phytoplankton and microorganisms in the bottom waters due to the cold temperature in early spring, and light limitation with high bottom turbidity in March (indicated by high TSS, Tables S1–S3). Interestingly, our $\delta^{18}O_P$ data suggest that in addition to the rapid P turnover in the surface water, P is substantially cycled by organisms even in deeper waters (Figure 7): $\delta^{18}O_P$ values below pycnocline (BP: 12–22 m) and in the bottom waters (B: 23–31 m) were close to equilibrium values (except in September at site 5.2 for BP, and in March for B; see discussion above for the deviations from equilibrium). This may suggest rapid biological P turnover and complete oxygen isotope equilibration [*Colman et al.*, 2005]. While previous studies in the Bay focused on nutrient limitation in the surface water (~ 0.5 m) [e.g., *Fisher et al.*, 1992; *Fisher et al.*, 1999; *Malone et al.*, 1996; *Prasad et al.*, 2010], substantial biomass is synthesized in the deeper euphotic zone as well where nutrient concentrations are high (Figure 2), and the nutrient limitation status differs from that in the surface (Figure 3 and discussion above). The regenerated P (via P remobilization and remineralization) (Figure 2) may also be extensively utilized to support primary productivity in the local deeper waters prior to their export to the surface water.

5. Conclusions

Our analyses of the PC:PN:PP ratio, APase activity, and phosphate oxygen isotope composition suggest strong seasonal and spatial (both lateral and vertical) variability in P availability and limitation in the Bay. Phosphate oxygen isotopic compositions identify the remobilization of terrestrial inorganic P (indicated by heavier than equilibrium values of $\delta^{18}O_P$) and remineralization of organic matter (suggested by lighter than equilibrium $\delta^{18}O_P$ values) as important sources of dissolved inorganic P. Phosphorus is utilized and cycled and thus isotopically equilibrated with ambient water by biological P turnover and well correlated with the degree of P limitation. Although most biological P uptake occurs in the surface layers where DIP is low, P regeneration from organic matter that sustains the high P levels in the deep waters is also extensively utilized and cycled to support biomass synthesis in the deeper euphotic zone. Efforts on understanding of P supply in the Bay therefore should focus attention beyond P stoichiometry in the surface waters. Together, these methods and approaches are important in understanding the temporal and spatial variability in P sources, limitation, and biological turnover in the Chesapeake Bay and provide useful insights for understanding P availability and its controls on primary productivity in similar coastal eutrophic environments.

Acknowledgments

We thank Debbie McKay, Kristen Heyer, Laura Fabian, and others at the Maryland Department of Natural Resources, Rick Younger, and the crew of R/V *Kerhin* for help with sample acquisition and sharing the shipboard data. We are very thankful to the Chesapeake Bay program for sharing the water column geochemistry data. We acknowledge Lisa Stout, Ha Vu, Nirman Dhakal, Mingjing Sun, Dengjun Wang, Hui Li, Qiang Li, and Balakrishna Avula for help processing unusually large volume of water samples. The work has been supported by grants from the U.S. Department of Agriculture (2015-67020 and 2016-08499) and National Science Foundation (1301765 and 1654642). All CBP data were obtained freely from the CBP Data Hub (http://www.chesapeakebay.net/data). Supporting data are included as three tables in a supporting information file; any additional data may be obtained from J.L. (e-mail: lijiying@udel.edu). We thank the two anonymous reviewers for comments that helped improved the manuscript.

References

Adams, M. M., M. R. Gómez-García, A. R. Grossman, and D. Bhaya (2008), Phosphorus deprivation responses and phosphonate utilization in a thermophilic Synechococcus sp. from microbial mats, *J. Bacteriol., 190*, 8171–8184.

Ator, S. W., and J. M. Denver (2015), Understanding nutrients in the Chesapeake Bay watershed and implications for management and restoration: The Eastern Shore*Rep. 2330-5703*, U.S. Geological Survey.

Bear, K. (2016), Tracking sources of particulate phosphorus in river waters: A case study in East Creak, a Chesapeake Bay watershed, Univ. of Delaware.
Biggs, R. B. (1970), Sources and distribution of suspended sediment in northern Chesapeake Bay, *Mar. Geol.*, *9*(3), 187–210.
Blake, R. E., J. O'neil, and G. A. Garcia (1997), Oxygen isotope systematics of biologically mediated reactions of phosphate: I. Microbial degradation of organophosphorus compounds, *Geochim. Cosmochim. Acta*, *61*(20), 4411–4422.
Blake, R. E., J. R. O'Neil, and G. A. Garcia (1998), Enzyme-catalyzed oxygen isotope exchange between inorganic phosphate and water: Reaction rates and temperature dependence at 5.7–30 C, *Mineral. Mag.*, *62*, 163–164.
Blake, R. E., J. R. O'Neil, and A. V. Surkov (2005), Biogeochemical cycling of phosphorus: Insights from oxygen isotope effects of phosphoenzymes, *Am. J. Sci.*, *305*(6-8), 596–620.
Boicourt, W. C., M. Kuzmić, and T. S. Hopkins (1999), The inland sea: Circulation of Chesapeake Bay and the Northern Adriatic, in *Ecosystems at the Land-Sea Margin: Drainage Basin to Coastal Sea*, edited by T. C. Malone et al., pp. 81–129, AGU, Washington, D. C.
Boynton, W. R., J. H. Garber, R. Summers, and W. M. Kemp (1995), Inputs, transformation, and transport of nitrogen and phosphorus in Chesapeake Bay and selected tributaries, *Estuaries*, *18*(1B), 285–314.
Chang, S. J., and R. E. Blake (2015), Precise calibration of equilibrium oxygen isotope fractionations between dissolved phosphate and water from 3 to 37°C, *Geochim. Cosmochim. Acta*, *150*, 314–329.
Chesapeake Bay Program (2012), Guide to using Chesapeake Bay program water quality monitoring data, United States Environmental Protection Agency, Annapolis, Available at: http://www.chesapeakebay.net/documents/3676/wq_data_userguide_10feb12_mod.pdf.
Colman, A. S., R. E. Blake, D. M. Karl, M. L. Fogel, and K. K. Turekian (2005), Marine phosphate oxygen isotopes and organic matter remineralization in the oceans, *Proc. Natl. Acad. Sci. U.S.A.*, *102*(37), 13,023–13,028.
Conley, D. J., W. M. Smith, J. C. Cornwell, and T. R. Fisher (1995), Transformation of particle-bound phosphorus at the land sea interface, *Estuarine Coastal Shelf Sci.*, *40*(2), 161–176.
Downing, J. A., S. B. Watson, and E. McCauley (2001), Predicting cyanobacteria dominance in lakes, *Can. J. Fish. Aquat. Sci.*, *58*(10), 1905–1908.
Duhamel, S., S. T. Dyhrman, and D. M. Karl (2010), Alkaline phosphatase activity and regulation in the North Pacific Subtropical Gyre, *Limnol. Oceanogr.*, *55*(3), 1414–1425.
Elsbury, K. E., A. Paytan, N. E. Ostrom, C. Kendall, M. B. Young, K. McLaughlin, M. E. Rollog, and S. Watson (2009), Using oxygen isotopes of phosphate to trace phosphorus sources and cycling in Lake Erie, *Environ. Sci. Technol.*, *43*(9), 3108–3114.
Fisher, T. R., E. R. Peele, J. W. Ammerman, and L. W. Harding (1992), Nutrient limitation of phytoplankton in Chesapeake Bay, *Mar. Ecol. Prog. Ser.*, *82*(1), 51–63.
Fisher, T. R., A. B. Gustafson, K. Sellner, R. Lacouture, L. W. Haas, R. L. Wetzel, R. Magnien, D. Everitt, B. Michaels, and R. Karrh (1999), Spatial and temporal variation of resource limitation in Chesapeake Bay, *Mar. Biol.*, *133*(4), 763–778.
Geider, R. J., and J. La Roche (2002), Redfield revisited: Variability of C:N:P in marine microalgae and its biochemical basis, *Eur. J. Phycol.*, *37*(1), 1–17.
Glibert, P. M., D. Fullerton, J. M. Burkholder, J. C. Cornwell, and T. M. Kana (2011), Ecological stoichiometry, biogeochemical cycling, invasive species, and aquatic food webs: San Francisco estuary and comparative systems, *Rev. Fish. Sci.*, *19*(4), 358–417.
Goldhammer, T., B. Brunner, S. M. Bernasconi, T. G. Ferdelman, and M. Zabel (2011), Phosphate oxygen isotopes: insights into sedimentary phosphorus cycling from the Benguela upwelling system, *Geochim. Cosmochim. Acta*, *75*(13), 3741–3756.
Gooddy, D. C., D. J. Lapworth, S. A. Bennett, T. H. Heaton, P. J. Williams, and B. W. Surridge (2016), A multi-stable isotope framework to understand eutrophication in aquatic ecosystems, *Water Res.*, *88*, 623–633.
Gross, A., A. Nishri, and A. Angert (2013), Use of phosphate oxygen isotopes for identifying atmospheric-P sources: A case study at Lake Kinneret, *Environ. Sci. Technol.*, *47*(6), 2721–2727.
Hagy, J. D., W. R. Boynton, C. W. Keefe, and K. V. Wood (2004), Hypoxia in Chesapeake Bay, 1950–2001: Long-term change in relation to nutrient loading and river flow, *Estuaries*, *27*(4), 634–658.
Hartzell, J. L. (2009), The fate of phosphorus along estuarine salinity gradients, PhD thesis, George Mason Univ.
Jaisi, D. P., and R. E. Blake (2014), Advances in using oxygen isotope ratios of phosphate to understand phosphorus cycling in the environment, *Adv. Agron.*, *125*, 1–53.
Jaisi, D. P., R. E. Blake, and R. K. Kukkadapu (2010), Fractionation of oxygen isotopes in phosphate during its interactions with iron oxides, *Geochim. Cosmochim. Acta*, *74*(4), 1309–1319.
Jaisi, D. P., R. K. Kukkadapu, L. M. Stout, T. Varga, and R. E. Blake (2011), Biotic and abiotic pathways of phosphorus cycling in minerals and sediments: Insights from oxygen isotope ratios in phosphate, *Environ. Sci. Technol.*, *45*(15), 6254–6261.
Jilbert, T., C. P. Slomp, B. G. Gustafsson, and W. Boer (2011), Beyond the Fe-P-redox connection: Preferential regeneration of phosphorus from organic matter as a key control on Baltic Sea nutrient cycles, *Biogeosciences*, *8*(6), 1699–1720.
Joshi, S. R. (2016), Biogeochemical cycling of phosphorus in the Chesapeake Bay and its watershed: Insights from phosphate oxygen isotope ratios, Univ. of Delaware.
Joshi, S. R., R. K. Kukkadapu, D. J. Burdige, M. E. Bowden, D. L. Sparks, and D. P. Jaisi (2015), Organic matter remineralization predominates phosphorus cycling in the mid-Bay sediments in the Chesapeake Bay, *Environ. Sci. Technol.*, *49*(10), 5887–5896.
Karl, D. M., and G. Tien (1992), MAGIC: A sensitive and precise method for measuring dissolved phosphorus in aquatic environments, *Limnol. Oceanogr.*, *37*(1), 105–116.
Keefe, C. W. (1994), The contribution of inorganic- compounds to the particulate carbon, nitrogen, and phosphorus in suspended matter and surface sediments of Chesapeake Bay, *Estuaries*, *17*(1B), 122–130.
Kemp, W. M., et al. (2005), Eutrophication of Chesapeake Bay: Historical trends and ecological interactions, *Mar. Ecol. Prog. Ser.*, *303*, 1–29.
Klausmeier, C. A., E. Litchman, T. Daufresne, and S. A. Levin (2004), Optimal nitrogen-to-phosphorus stoichiometry of phytoplankton, *Nature*, *429*(6988), 171–174.
Kolodny, Y., B. Luz, and O. Navon (1983), Oxygen isotope variations in phosphate of biogenic apatites. 1. Fish bone apatite—Rechecking the rules of the game, *Earth Planet. Sci. Lett.*, *64*(3), 398–404.
Lécuyer, C., P. Grandjean, and C. Emig (1996), Determination of oxygen isotope fractionation between water and phosphate from living lingulids: Potential application to palaeoenvironmental studies, *Palaeogeogr. Palaeoclimatol. Palaeoecol.*, *126*(1), 101–108.
Liang, Y., and R. Blake (2006a), Oxygen isotope signature of P i regeneration from organic compounds by phosphomonoesterases and photooxidation, *Geochim. Cosmochim. Acta*, *70*(15), 3957–3969.
Liang, Y., and R. Blake (2006b), Oxygen isotope composition of phosphate in organic compounds: Isotope effects of extraction methods, *Org. Geochem.*, *37*(10), 1263–1277.
Liang, Y., and R. E. Blake (2007), Oxygen isotope fractionation between apatite and aqueous-phase phosphate: 20–45°C, *Chem. Geol.*, *238*(1), 121–133.

Liang, Y., and R. E. Blake (2009), Compound-and enzyme-specific phosphodiester hydrolysis mechanisms revealed by $\delta^{18}O$ of dissolved inorganic phosphate: implications for marine P cycling, *Geochim. Cosmochim. Acta*, *73*(13), 3782–3794.

Longinelli, A., and S. Nuti (1973), Revised phosphate-water isotopic temperature scale, *Earth Planet. Sci. Lett.*, *19*(3), 373–376.

Malone, T. C., D. J. Conley, T. R. Fisher, P. M. Glibert, L. W. Harding, and K. G. Sellner (1996), Scales of nutrient-limited phytoplankton productivity in Chesapeake Bay, *Estuaries*, *19*(2B), 371–385.

McLaughlin, K., B. J. Cade-Menun, and A. Paytan (2006a), The oxygen isotopic composition of phosphate in Elkhorn Slough, California: A tracer for phosphate sources, *Estuarine Coastal Shelf Sci.*, *70*(3), 499–506.

McLaughlin, K., A. Paytan, C. Kendall, and S. Silva (2006b), Oxygen isotopes of phosphatic compounds—Application for marine particulate matter, sediments and soils, *Mar. Chem.*, *98*(2), 148–155.

McLaughlin, K., F. Chavez, J.T. Pennington, and A. Paytan (2006c), A time series investigation of the oxygen isotopic composition of dissolved inorganic phosphate in Monterey Bay, California, *Limnol. Oceanogr.*, *51*(5), 2370.

McLaughlin, K., J. A. Sohm, G. A. Cutter, M. W. Lomas, and A. Paytan (2013), Phosphorus cycling in the Sargasso Sea: Investigation using the oxygen isotopic composition of phosphate, enzyme-labeled fluorescence, and turnover times, *Global Biogeochem Cycles*, *27*, 375–387, doi:10.1002/gbc.20037.

Nicholson, D., S. Dyhrman, F. Chavez, and A. Paytan (2006), Alkaline phosphatase activity in the phytoplankton communities of Monterey Bay and San Francisco Bay, *Limnol. Oceanogr.*, *51*(2), 874–883.

North, R. L., S. J. Guildford, R. E. H. Smith, S. M. Havens, and M. R. Twiss (2007), Evidence for phosphorus, nitrogen, and iron colimitation of phytoplankton communities in Lake Erie, *Limnol. Oceanogr.*, *52*(1), 315–328.

O'Neil, J. R., L. J. Roe, E. Reinhard, and R. E. Blake (1994), A rapid and precise method of oxygen isotope analysis of biogenic phosphate, *Isr. J. Earth Sci.*, *43*(3–4), 203–212.

Paytan, A., and K. McLaughlin (2011), Tracing the sources and biogeochemical cycling of phosphorus in aquatic systems using isotopes of oxygen in phosphate, *Handbook Environ. Isot. Geochem., 1 and 2*, 419–436.

Paytan, A., Y. Kolodny, A. Neori, and B. Luz (2002), Rapid biologically mediated oxygen isotope exchange between water and phosphate, *Global Biogeochem Cycles*, *16*(1), 1013, doi:10.1029/2001GB001430.

Prasad, M. B. K., M. R. P. Sapiano, C. R. Anderson, W. Long, and R. Murtugudde (2010), Long-term variability of nutrients and chlorophyll in the Chesapeake Bay: A retrospective analysis, 1985–2008, *Estuaries Coasts*, *33*(5), 1128–1143.

Pritchard, D. W. (1956), The dynamic structure of a coastal plain estuary, *J. Mar. Res.*, *15*, 33–42.

Pritchard, D. W. (1967), Observations of circulation in coastal plain estuaries, in *Estuaries*, *AAS Publ.*, vol. 83, edited by G. H. Lauff, pp. 37–44, Am. Acad. of Sci., Washington, D. C.

Redfield, A. C. (1958), The biological control of chemical factors in the environment, *Am. Sci.*, *46*(3), 205–221.

Reynolds, C. S. (1999), Non-determinism to Probability, or N: P in the community ecology of phytoplankton, *Arch. Hydrobiol.*, *146*(1), 23–35.

Sterner, R. W., and J. J. Elser (2002), *Ecological Stoichiometry: The Biology of Elements From Molecules to the Biosphere*, Princeton Univ. Press, Princeton.

Stout, L. M., S. R. Joshi, T. M. Kana, and D. P. Jaisi (2014), Microbial activities and phosphorus cycling: An application of oxygen isotope ratios in phosphate, *Geochim. Cosmochim. Acta*, *138*, 101–116.

Sun, M., J. Alikhani, A. Massoudieh, R. Greiner, and D. P. Jaisi (2017), Phytate degradation by different phosphohydrolase enzymes: Contrasting kinetics, decay rates, pathways, and isotope effects, *Soil Sci. Soc. Am. J.*, *81*, 61–75.

Suttle, C., and P. Harrison (1988), Ammonium and phosphate uptake rates, N: P supply ratios, and evidence for N and P limitation in some oligotrophic lakes, *Limnol. Oceanogr.*, *33*(2), 186–202.

Tamburini, F., S. M. Bernasconi, A. Angert, T. Weiner, and E. Frossard (2010), A method for the analysis of the delta O-18 of inorganic phosphate extracted from soils with HCl, *Eur. J. Soil Sci.*, *61*(6), 1025–1032.

Thomson-Bulldis, A., and D. Karl (1998), Application of a novel method for phosphorus determinations in the oligotrophic North Pacific Ocean, *Limnol. Oceanogr.*, *43*(7), 1565–1577.

von Sperber, C., F. Tamburini, B. Brunner, S. M. Bernasconi, and E. Frossard (2015), The oxygen isotope composition of phosphate released from phytic acid by the activity of wheat and *Aspergillus niger* phytase, *Biogeosciences*, *12*(13), 4175–4184.

Young, M. B., K. McLaughlin, C. Kendall, W. Stringfellow, M. Rollog, K. Elsbury, E. Donald, and A. Paytan (2009), Characterizing the oxygen isotopic composition of phosphate sources to aquatic ecosystems, *Environ. Sci. Technol.*, *43*(14), 5190–5196.

Zhang, X., M. Roman, D. Kimmel, C. McGilliard, and W. Boicourt (2006), Spatial variability in plankton biomass and hydrographic variables along an axial transect in Chesapeake Bay, *J. Geophys. Res.*, *111*, C05S11, doi:10.1029/2005JC003085.